

# Physikalisch-Technische Bundesanstalt, Germany

## Report on Activities to the 17<sup>th</sup> Session of the Consultative Committee for Time and Frequency, September 2006

This report covers the activities pursued in PTB concerning

1. primary clocks
2. atomic-time scales
3. time and frequency comparisons
4. optical frequency standards/clocks
5. optical frequency measurements.

### 1. Primary clocks

#### 1.1 Fountain clock CSF1

CSF1 is a caesium fountain clock using the (100)-geometry of the laser beams for the capture of caesium atoms in a magneto-optical trap. After a molasses phase the atoms traverse a state-selection cavity before reaching the main microwave cavity and continuing the ballistic flight. CSF1 has been operated almost every day over the last five years. Most of the time, CSF1 is run under a variety of operating conditions, with the aim of investigating possible systematic effects. CSF1 is still in the process of further optimisation and modernisation of the control and detection electronics and software.

Since CSF1 became operational, it was run 15 times under routine operating conditions for periods of 15-25 days each. The results were submitted to BIPM and served for the measurement of the TAI scale unit [1]. At the time the CSF1  $\mu_B$  was estimated as  $\leq 1 \cdot 10^{-15}$  [2].

In November 2004 during a frequency comparison campaign [3] between several European fountains relative frequency variations of CSF1 of the order of  $10^{-14}$  became apparent. These frequency variations could be traced back to Majorana-transitions caused by unintended changes of the properties of the magnetic shields [4]. By proper current settings of correction coils located close to the lower shield caps the problem could be remedied.

Another effect was encountered already before, when the main cavity was operated at increased microwave power: Application of, e.g.,  $3\pi/2$ -pulses to the atoms instead of  $1\pi/2$ -pulses leads to a shift of the fountain output frequency of 5 parts in  $10^{15}$ . Recently we found evidence for a cause of this effect in the treatment of the collisional shift, although we will have to run more experiments to determine whether the frequency difference has disappeared completely.

The intensive search for the origin of the frequency changes at increased microwave power is the reason that no CSF1 measurements of the TAI scale unit have been submitted to BIPM over a two-year period. Many possible sources of this effect were investigated with some concentration on Majorana transitions [4] and microwave leakage [5], resulting in a deeper understanding of many aspects of the physics of fountain frequency standards.

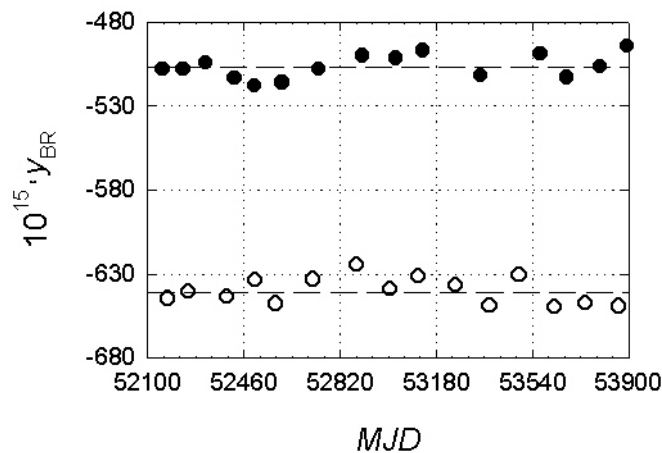
In summer 2005 and in summer 2006 CSF1 was again used as a reference for absolute measurements of the 435.5 nm  $^{171}\text{Yb}^+$ -clock transition frequency. This transition has been recommended as a secondary representation of the second by the CCL/CCTF Joint Working

Group on Secondary Representations of the Second [6]. A detailed report on the  $^{171}\text{Yb}^+$  frequency measurements is given in Appendix 1. Due to the unresolved issue associated with the operation of CSF1 at increased microwave power, its estimated type-B uncertainty was raised to  $2.65 \cdot 10^{-15}$  in the  $^{171}\text{Yb}^+$  absolute frequency measurements. This uncertainty estimate is based on the frequency difference observed between frequency measurements applying either  $1\pi/2$ -pulses or  $3\pi/2$ -pulses to the CSF1 main cavity and using the  $^{171}\text{Yb}^+$ -clock transition frequency as a reference.

### 1.2 Fountain clock CSF2

CSF2 is a caesium fountain clock using the (111)-geometry of the laser beams for the capture of caesium atoms directly in an optical molasses using large-diameter laser beams. This fountain clock differs in a number of constructional details from CSF1, as reported in [7].

Early in 2006, the setup of CSF2 was completed. An initial two-week run as a frequency standard went very well, with a short-term stability of several parts in  $10^{13}$  at one second of integration time and a difference of its raw output frequency (i.e., no corrections for systematics applied) with respect to CSF1 that is consistent with the difference in C-fields between the two fountain clocks (100 nT in CSF1 vs. 140 nT in CSF2) [7]. A thorough optimization of operating parameters and a full characterization of possible frequency biases is in progress.



*Results of beam reversals performed on CS1(o) and CS2 (●) during the last five years.*

### 1.3 Thermal beam clocks

The primary clocks CS1 and CS2 have been continuously operated during the last years. Measurements of parameters affecting the clock frequency, like mean atomic velocity, magnetic field, cavity phase difference, spectral purity of the microwave interrogation signal, servo electronic offsets, and temperature of the vacuum enclosure, were performed. They supported the validity of the previous estimates of the clocks' uncertainties  $u_B$  of  $7 \cdot 10^{-15}$  and  $12 \cdot 10^{-15}$ , for CS1 and CS2, respectively [8]. As a detail we show the results of the beam reversals performed during the last five years, expressed by the beam reversal frequency shift  $y_{BR}$ . It is a measure for the stability of the end-to-end cavity phase shift and the reproducibility of the beam reversal procedures. The scatter of data can be well explained by shot-noise limited performance of CS1 and CS2 and the available frequency references.

In view of the superiority of the fountain type clocks we abandoned operation of CS4 and display it now in a local museum. CS3 has been operated almost continuously but is treated like any of PTB's commercial clocks.

## **2. Time Scales**

PTB continues to realize UTC(PTB) from the 5 MHz output of CS2 and an associated phase micro stepper (UTC(PTB) whose rate being adjusted in steps of 0.5 ns/d at the end of a month if required to keep the time scale in reasonable agreement with UTC. The steering values are published in PTB's Time Service Bulletin.

We have studied the possibility to realize UTC(PTB) based on the output frequency of a hydrogen maser steered towards the frequency of CSF1. Earlier tests revealed that the stability and predictability of the PTB masers and the performance of the hardware components did not allow a substantial improvement over the current procedures. In the meantime new hardware components were installed for the generation and distribution of UTC(PTB) signals as well as for a fountain based time scale. Studies in this direction will be resumed as soon as fountain data will be available more reliably.

## **3. Time and Frequency Comparisons**

Different GPS common view (CV) time transfer evaluation techniques and Two-Way Satellite Time and Frequency Transfer (TWSTFT) have been employed in the realization of TAI by BIPM. In this context PTB provides data of one single-channel, of one C/A code multi-channel, and of a geodetic time-oriented GPS receiver as well as TWSTFT data. A new multi-channel combined GPS / GLONASS receiver has been installed. During the third quarter of 2006 its data will be made available on a daily basis. Additionally, a Turbo Rogue SNR 12 RM which is on loan from NIST is operated for studies of carrier phase GPS frequency transfer between NIST and PTB. Data were used in the earlier frequency comparisons between NIST-F1 and CSF1, and this usage shall be resumed.

During the last two years, PTB has upgraded its TWSTFT capabilities. Operation of the older single-channel Satre modem is now fully automatic and allows participation in the bi-hourly comparisons using Intelsat IS-307 in Ku-band with INRiM, LNE-SYRTE, METAS, NIST, NPL, OCA, ROA, SP, TUG, USNO, and VSL. A new multi-channel Satre modem allowing for the use of more PRN codes and simultaneous reception and processing of two remote signals at a time has been integrated in the measurement routines and is currently being tested.

A second completely independent TWSTFT link has been established between USNO and PTB, with transponder frequencies in the X-band. The routine Ku-band link has some strategic importance, since currently it connects almost one half of the atomic clocks in the BIPM network that are employed for the realization of TAI. The X-band data are provided as a backup. Initially, part of the station operated at PTB was on loan from USNO, meanwhile PTB invested in new components to improve the reliability of the link. We are currently preparing the provision of the time transfer data UTC(PTB) UTC(USNO) on a daily basis on the PTB ftp server.

NICT has stimulated the installation of a TWSTFT link between NICT and PTB. This link allows connection between institutes in USA, Europe, and the Asian Pacific region using

TWSTFT only. Specific features of the architecture of the Earth stations are the use of the multi-channel time-transfer modems developed by NICT, which are also in operation in the Asia-Pacific TWSTFT network, and optical fiber connections for radio frequency transmission between indoor and outdoor equipment. Especially at PTB a distance of 1 km has to be bridged in this way. Frequency comparisons demonstrated a significant improvement compared to the GPS based comparisons made hitherto [9]. The causes of diurnal variations appearing in the measurements are still under research. In the meantime, also KRISS is performing TWSTFT with PTB using the satellite Pan-Am Sat PAS-4. It is PTB's proposal to establish a network of TWSTFT comparisons between European institutes and those in the Asia-Pacific region and share the cost for the transponder lease. These costs have up to now been carried generously by NICT alone.

Reaching uncertainty levels of time transfer well below 1 ns will require that the instability of the links itself is better understood. We observe annual variations between the Ku-band and X-band links at the same level as the current calibration uncertainty. We also observe variations of the measurement precision for a TWSTFT link in dependence of the traffic on the satellite transponder but also without clear correlation with known parameters. It is hoped that TWSTFT can be continued on a stable basis not only for occasional time scale comparisons but also for research in the causes of observed deficiencies of the method. Otherwise comparisons of the best primary clocks and possibly also of optical frequency standards at their uncertainty level would remain essentially impossible.

Calibration activities 2004-2006:

GPS:

C/A: Four calibrations using the travelling BIPM C/A-code receiver in 2003-06, 2003-09, 2004-07, 2005-10, one calibration in the framework of EUROMET project 529 (organized by ROA).

TAIP3:

Two calibrations with Z12-T from BIPM (June 2004, June/July 2006).

TWSTFT:

Three calibration exercises of Ku-band links were performed, involving the following institutes:

No.	Year	Participating Institutes	Reference
1	2004	PTB-VSL-OP-NPL-PTB	Piester et al. [10]
2	2005	PTB-SP-VSL-NPL-OP-INRIM-PTB	Piester et al. [11]
3	2006	TUG-PTB-METAS-TUG	to be published

Calibration constants with estimated uncertainties down to 0.9 ns were achieved. In the 2005 campaign, the first recalibration of some TWSTFT time links was performed, and the average reproducibility of 0.97 ns is consistent with the estimated uncertainties of the links and of the calibration values [11].

Four calibrations of the X-band link were carried out by USNO in March and September 2004, May 2005, and April 2006. The repeated calibration exercises show very good reproducibility of the combined estimated uncertainties at or even below the 1 nanosecond level [12].

#### 4. Optical Frequency Standards – Optical Clocks

PTB operates an optical frequency standard based on the 657 nm  $^1S_0 - ^3P_1$  transition ( $f = 455.986$  THz) in an ultracold ( $T \approx 15$   $\mu$ K) ballistically expanding atomic cloud of calcium atoms. A possible fractional uncertainty of  $2 \cdot 10^{-15}$  and an instability of  $\sigma_y \approx 6 \cdot 10^{-16} (\tau/s)^{-1/2}$  in the measurements that are currently underway were estimated [13]. Frequency shifts due to non-ideal characteristics of acousto-optic modulators were identified [14]. Further progress using freely expanding absorbers will require high efforts. Thus the future work concentrates on using strontium atoms for an optical lattice clock. So far we obtain about  $10^7$   $^{88}\text{Sr}$  atoms at 1  $\mu$ K within a cooling time of a few milliseconds. The laser for the optical lattice is available and the 698 nm clock laser is currently being set up. We expect first frequency measurements within this year. For these standards the frequency noise of the interrogation laser limits the achievable stability. A diode laser system with a laser linewidth of 1 Hz has been developed [15]. To further reduce the linewidth the noise due to the coupling of vibrations to the reference cavity had to be reduced. A novel vibration insensitive mounting configuration has been developed that reduced the influence by at least one order of magnitude [16] and can be used also in transportable optical standards.

The most advanced optical frequency standard at PTB is based on the  $^{171}\text{Yb}^+$  single ion transition with a frequency of 688 THz (see Appendix 1).

#### 5. Optical Frequency Measurements

For optical frequency standards PTB develops fiber-based frequency comb generators for use in transportable and long-term stable optical clocks. In co-operation with the University of Konstanz we have implemented a self-referenced frequency comb generator based on a femtosecond fiber laser and demonstrated the first long-term optical frequency measurement, lasting 88 h [17]. We tested the accuracy of fiber-laser based frequency combs by performing direct frequency comb comparisons. In a first experiment in co-operation with the University of Konstanz and the Max Planck Institute for Quantum Optics München, a stable optical frequency near 1545 nm was simultaneously measured by two independent comb systems, giving an agreement to within  $6 \times 10^{-16}$  [18]. In more recent experiments, we obtained an agreement to within a few parts in  $10^{-17}$  for long-term measurements of the  $\text{Yb}^+$  ion transition, as well as for a stable optical frequency near 1545 nm [19].

We measured the ratio of two optical frequencies: employing a frequency comb as transfer oscillator, we synthesised a well-defined ultra-stable optical frequency near 194 THz (1545 nm) from a spectroscopy laser near 344 THz (871 nm), which is used in the  $\text{Yb}^+$  ion optical frequency standard. The ratio of these two optical frequencies was simultaneously measured by two fiber comb systems. We deduce from the results that the uncertainty for the optical frequency ratio measurement was below  $7 \times 10^{-18}$  [19].

#### References

- [1] P. Wolf, G. Petit, E. Peik, C. Tamm, H. Schnatz, B. Lipphardt, S. Weyers, R. Wynands, J.-Y. Richard, S. Bize, F. Chapelet, F. Ferreira dos Santos, A. Clairon, Proc. 20th European Frequency and Time Forum (EFTF), Braunschweig, March 2006, 476-485
- [2] S. Weyers, A. Bauch, R. Schröder and Chr. Tamm, Proc. 6<sup>th</sup> Symposium on Frequency Standards and Metrology, St. Andrews, Sept. 2001, 64 – 71
- [3] A. Bauch, J. Achkar, S. Bize, D. Calonico, R. Dach, R. Hlavac, L. Lorini, T. Parker, G. Petit, D. Piester, K. Szymaniec and P. Urich, Metrologia 43, 109 – 120 (2006)

- [4] S. Weyers, R. Schröder, and R. Wynands, Proc. 20th European Frequency and Time Forum (EFTF), Braunschweig, March 2006, 219-223
- [5] S. Weyers, R. Schröder, and R. Wynands, Proc. 20th European Frequency and Time Forum (EFTF), Braunschweig, March 2006, 173-180
- [6] P. Gill and F. Riehle, Proc. 20th European Frequency and Time Forum (EFTF), Braunschweig, March 2006, 282-288
- [7] R. Wynands, D. Griebisch, R. Schröder, and S. Weyers, Proc. 20th European Frequency and Time Forum (EFTF), Braunschweig, March 2006, 200-202
- [8] T. Heindorff, A. Bauch, P. Hetzel, G. Petit, S. Weyers, Metrologia, **38**, 2001, 497- 502
- [9] H. Maeno, M. Fujieda, D. Piester, A. Bauch, M. Aida, Q. T. Lam, T. Gotoh, and Y. Takahashi, Proc. 20th European Frequency and Time Forum - EFTF 2006, Braunschweig, Germany, March 2006, 575-579
- [10] D. Piester, R. Hlavac, J. Achkar, G. de Jong, B. Blanzano, H. Ressler, J. Becker, P. Merck, O. Koudelka, Proc. 19th European Frequency and Time Forum - EFTF 2005, Besancon, France, March 2005, 354-359
- [11] D. Piester, J. Achkar, J. Becker, B. Blanzano, K. Jaldehag, G. de Jong, O. Koudelka, L. Lorini, H. Ressler, M. Rost, I. Sesia, and P. Whibberley, Proc. 20th European Frequency and Time Forum - EFTF 2006, Braunschweig, Germany, March 2006, 460-467
- [12] D. Piester, A. Bauch, J. Becker, T. Polewka, A. McKinley, L. Breakiron, A. Smith, B. Fonville, D. Matsakis, Proc. 2005 Joint IEEE International Frequency Control Symposium and Precise Time and Time Interval Systems and Applications Meeting, Vancouver, BC, Canada, Aug 2005, 316-323
- [13] C. Degenhardt, H. Stoehr, C. Lisdat, G. Wilpers, H. Schnatz, B. Lipphardt, T. Nazarova, P. Pottie, U. Sterr, J. Helmcke and F. Riehle, Phys. Rev. A 72, 2005, 062111-1-17
- [14] C. Degenhardt, T. Nazarova, C. Lisdat, H. Stoehr, U. Sterr and F. Riehle, IEEE Trans. Instrum. Meas. 54, 2005, 771-775
- [15] H. Stoehr, F. Mensing, J. Helmcke and U. Sterr, Opt. Lett. 31, 2006, 736-738
- [16] T. Nazarova, F. Riehle and U. Sterr, Appl. Phys. B 83, 2006, 531-536
- [17] F. Adler, K. Moutzouris, A. Leitenstorfer, H. Schnatz, B. Lipphardt, G. Grosche, and F. Tauser, Opt. Express **12** (24), 2004, 5872-5880
- [18] P. Kubina, P. Adel, F. Adler, G. Grosche, T.W. Hänsch, R. Holzwarth, A. Leitenstorfer, B. Lipphardt, H. Schnatz, Opt. Express Vol. 13 (3), 2005, 904-909
- [19] G. Grosche, B. Lipphardt, H. Schnatz, Proc. CPEM (2006)

## Appendix 1

Physikalisch-Technische Bundesanstalt, Germany

July 2006

### Report on recent frequency measurements of the 436 nm $^2S_{1/2}(F=0) - ^2D_{3/2}(F=2)$ transition of $^{171}\text{Yb}^+$

#### (i) General conditions of measurement

In an extension of earlier work [1-3], five frequency measurements of the 688 THz (436 nm) transition of  $^{171}\text{Yb}^+$  were performed in July and August 2005 and in June 2006. The output of a frequency-doubled diode laser was locked to the  $^2S_{1/2}(F=0) - ^2D_{3/2}(F=2)$  transition of a single  $^{171}\text{Yb}^+$  ion confined in a Paul trap. The diode laser frequency was compared to the caesium fountain clock CSF1 of PTB using a frequency comb generator based on a  $\text{Er}^{3+}$ -doped fiber laser [4].

Immediately before the measurement of Aug. 9, 2005, two  $^{171}\text{Yb}^+$  traps were operated simultaneously as described in [5] in order to compare the transition frequencies of the trapped ions for various orientations of the magnetic field. The results of this comparison confirm the results reported in [5].

The  $^{171}\text{Yb}^+$  trap was operated at room temperature ( $T=297$  K). The  $^{171}\text{Yb}^+$  transition frequency values reported here include the frequency shift due to the ambient blackbody radiation. Tabulated oscillator strength data and the atomic polarizability measurements described in [5,6] indicate that the blackbody AC Stark shift of the  $\text{Yb}^+$  reference transition is  $-0.37(5)$  Hz at  $T=300$  K.

#### (ii) Measurement results and uncertainty contributions

Notation:  $\nu_i(\text{Yb}^+) = 688\,358\,979\,309\,000$  Hz +  $x_i$  Hz,  $i$ : number of measurement

$i$	Starting Date	$x_i$ / Hz	$u_{A_i}$ / Hz	$u_{B}(\text{Cs})$ / Hz	$u_{B}(\text{Yb}^+)$ / Hz
1	05.07.05	307.84	3.43	1.82	1.05
2	06.07.05	307.51	0.46	1.82	1.05
3	09.08.05	307.49	1.01	1.82	1.05
4	10.08.05	307.07	0.64	1.82	1.05
5	22.06.06	307.70	0.44	1.82	1.05

Weighted mean of measured  $^{171}\text{Yb}^+ ^2S_{1/2}(F=0) - ^2D_{3/2}(F=2)$  transition frequencies:

**$\nu(\text{Yb}^+) = 688\,358\,979\,309\,307.47$  Hz**

Weighting proportional to  $(u_{A_i}^2 + u_{B_i}^2(\text{Cs}) + u_{B_i}^2(\text{Yb}^+))^{-1}$ . Earlier results [2,3] are not included because of their significantly higher uncertainties. Their inclusion would change the weighted mean by  $+0.16$  Hz.

Type A uncertainty of  $v(\text{Yb}^+)$ ,  $i=1\dots 5$ :

$$u_A = (\sum u_{Ai}^{-2})^{-1/2} = \mathbf{0.28 \text{ Hz}}$$

Type B uncertainty of  $v(\text{Yb}^+)$ ,  $i=1\dots 5$ :

$$u_B = (u_B^2(\text{Cs}) + u_B^2(\text{Yb}^+))^{1/2} = \mathbf{2.11 \text{ Hz}}$$

Combined uncertainty of  $v(\text{Yb}^+)$ ,  $i=1\dots 5$ :

$$u(\text{combined}) = (u_A^2 + u_B^2)^{1/2} = \mathbf{2.12 \text{ Hz}}$$

**(iii) Comments on some type B uncertainty contributions  
(see also enclosed GUM worksheet)**

(1) The value  $u_B(\text{Cs}) = 1.82 \text{ Hz}$  (corresponding to a fractional uncertainty of  $2.65 \cdot 10^{-15}$ ) takes into account an unresolved issue associated with the operation of CSF1 at increased microwave power (see 2006 report of PTB to CCTF, Sec. 1).

(2) The assumed quadrupole shift contribution to  $u_B(\text{Yb}^+)$  is a factor of two larger than the statistical uncertainty of the trap-trap-comparison measurements described in [4]. These comparisons did not show any statistically significant quadrupole or tensorial Stark shifts.

(3) The  $u_B(\text{Yb}^+)$  contributions taking into account the trap field-induced Stark shift and the relativistic Doppler shift correspond to a stray-field induced micromotion amplitude that is a factor of two larger than the maximum amplitude which might remain undetected with the employed compensation scheme for electrostatic stray fields [5,6]. The amplitude of the thermal secular motion is much smaller than the assumed micromotion amplitude.

(4) The blackbody shift contribution to  $u_B(\text{Yb}^+)$  is an estimate of possible deviations of the AC Stark shift from the purely scalar shift caused by isotropic 300 K blackbody radiation. Such deviations could be caused by spurious thermal radiation sources near the trap and by laser stray light. Tests of the mechanical shutters which block the cooling and repumping laser light during the clock laser pulse were carried out during the trap-trap comparison experiments (separate shutters are used for the two trap setups).

(5) The  $u_B(\text{Yb}^+)$  contribution taking into account the quadratic Zeeman shift caused by the rf trap drive current is based on an estimate of the displacement current through one octant of the trap electrode system and of the resulting magnetic field. In a perfectly symmetric trap, the magnetic field contributions of all octants would add up to zero at trap center. The magnetic field produced by other rf conductors is expected to be smaller than the assumed field since these conductors are located sufficiently far from trap center.

**References**

- [1] J. Stenger, Chr. Tamm, N. Haverkamp, S. Weyers, H.R. Telle, *Opt. Lett.* **26**, 1589 (2001)
- [2] T. Quinn, *Metrologia* **40**, 103 (2003)
- [3] E. Peik, B. Lipphardt, H. Schnatz, T. Schneider, Chr. Tamm, *Phys. Rev. Lett.* **93**, 170801 (2004)
- [4] Ph. Kubina, P. Adel, G. Grosche, Th. W. Hänsch, R. Holzwarth, B. Lipphardt, H. Schnatz, *Opt. Express* 904 (2005)
- [5] T. Schneider, E. Peik, Chr. Tamm, *Phys. Rev. Lett.* **94**, 230801 (2005)
- [6] T. Schneider, PhD thesis, Univ. Hannover (2005)
- [7] E. Peik, T. Schneider, Chr. Tamm, *J. Phys. B: At. Mol. Opt. Phys.* **39**, 145 (2006)

**GUM worksheet:**

**$^{171}\text{Yb}^+$  frequency standard, July/Aug. 2005 and June 2006 measurements, corrections and systematic uncertainty contributions**

**Model Equation:**

$$f_{\text{YbCorr}} = f_{2\text{ndZeem}} + f_{\text{grav}} + \delta Q\text{Shift} + \delta\text{Servo} + \delta\text{StarkBBDev} + \delta\text{StarkTrap} + \delta\text{relDopp};$$

$$f_{2\text{ndZeem}} = f_{\text{ZeemDC}} + f_{\text{ZeemAC}};$$

$$f_{\text{ZeemDC}} = s0 \cdot (B_{\text{DC}})^2;$$

$$f_{\text{ZeemAC}} = (s0/2) \cdot (B_{\text{AC}})^2;$$

$$f_{\text{grav}} = s3 \cdot h_{\text{refminusYb}}$$

**List of Quantities:**

Quantity	Unit	Definition
$f_{\text{YbCorr}}$	Hz	corrections to $f_{\text{Yb}}$ due to interactions of trapped ion
$f_{2\text{ndZeem}}$	Hz	time average of second-order Zeeman shift
$f_{\text{grav}}$	Hz	gravitational shift of measured frequency
$\delta Q\text{Shift}$	Hz	uncertainty due to stray-field induced quadrupole shift of Yb frequency
$\delta\text{Servo}$	Hz	uncertainty due to servo errors and spectral asymmetry of probe laser (see also Ref. [7])
$\delta\text{StarkBBDev}$	Hz	uncertainty due to deviation of the AC Stark shift from 300 K-blackbody shift; includes shift due to laser stray light
$\delta\text{StarkTrap}$	Hz	uncertainty due to quadratic Stark shift caused by secular motion and by excessive micromotion
$\delta\text{relDopp}$	Hz	uncertainty due to relativistic Doppler shift caused by secular motion and by excessive micromotion
$f_{\text{ZeemDC}}$	Hz	second-order Zeeman shift due to applied static magnetic field
$f_{\text{ZeemAC}}$	Hz	time average of second-order Zeeman shift due to magnetic field associated with rf trap drive
$s0$	Hz/T <sup>2</sup>	sensitivity coefficient of quadratic Zeeman shift
$B_{\text{DC}}$	T	static magnetic field at trap center
$B_{\text{AC}}$	T	amplitude of rf magnetic field at trap center
$s3$	Hz/m	gravitational shift coefficient of measured frequency
$h_{\text{refminusYb}}$	m	elevation difference of Cs reference and Yb+ standard

 **$f_{\text{YbCorr}}$ : Result**

total systematic shift of Yb+ single-ion standard

 **$f_{2\text{ndZeem}}$ : Interim Result** **$f_{\text{grav}}$ : Interim Result**

gravitational redshift difference due to different elevation of Cs clock and Yb+ standard

**$\delta Q_{\text{Shift}}$ : Stray-field induced quadrupole shift**

Type B normal distribution

Value: 0 Hz

Expanded Uncertainty: 1 Hz

Coverage Factor: 1

**$\delta \text{Servo}$ : Servo error**

Type B normal distribution

Value: 0 Hz

Expanded Uncertainty: 0.1 Hz

Coverage Factor: 1

**$\delta \text{StarkBBDev}$ : AC Stark shift minus 300 K blackbody shift**

Type B normal distribution

Value: 0 Hz

Expanded Uncertainty: 0.3 Hz

Coverage Factor: 1

**$\delta \text{StarkTrap}$ : Stark shift due to trap field**

Type B rectangular distribution

Value: 0 Hz

Halfwidth of Limits: 0.03 Hz

**$\delta \text{relDopp}$ : Relativistic Doppler shift due to micromotion and secular motion**

Type B rectangular distribution

Value: -0.01 Hz

Halfwidth of Limits: 0.01 Hz

**$f_{\text{ZeemDC}}$ : Interim Result**

**$f_{\text{ZeemAC}}$ : Interim Result**

**$s_0$ : Coefficient for quadratic Zeeman shift**

Type B normal distribution

Value:  $520 \cdot 10^8 \text{ Hz/T}^2$

Expanded Uncertainty:  $26 \cdot 10^8 \text{ Hz/T}^2$

Coverage Factor: 1

**$B_{\text{DC}}$ : Applied static magnetic field**

Type B normal distribution

Value:  $3.09 \cdot 10^{-6} \text{ T}$  (in 2005);  $2.76 \cdot 10^{-6} \text{ T}$  (in 2006)

Expanded Uncertainty:  $0.1 \cdot 10^{-6} \text{ T}$

Coverage Factor: 1

**$B_{\text{AC}}$ : AC magnetic field amplitude**

Type B rectangular distribution

Value:  $2 \cdot 10^{-8} \text{ T}$

Halfwidth of Limits:  $2 \cdot 10^{-8} \text{ T}$

**s3: Proportionality factor for gravitational redshift**

Type B rectangular distribution

Value: 0.0688 Hz/m (used in 2005); 0.0750 Hz/m (corrected, used in 2006)

Halfwidth of Limits:  $1 \cdot 10^{-6}$  Hz/m **$h_{\text{refminusYb}}$ : Effective elevation CSF1- elevation Yb+ trap**

Type B rectangular distribution

Value: -0.75 m

Halfwidth of Limits: 0.01 m

**Uncertainty Budget (2005 measurements):**

Quantity	Value	Standard Uncertainty	Degrees of Freedom	Sensitivity Coefficient	Uncertainty Contribution	Index
$f_{2\text{ndZeem}}$	0.4965 Hz	0.0406 Hz				
$f_{\text{grav}}$	-0.05160 Hz	$397 \cdot 10^{-6}$ Hz				
$\delta\text{QShift}$	0.0 Hz	1.00 Hz	50	1.0	1.0 Hz	90.7 %
$\delta\text{Servo}$	0.0 Hz	0.100 Hz	50	1.0	0.10 Hz	0.9 %
$\delta\text{StarkBBD}$ ev	0.0 Hz	0.300 Hz	50	1.0	0.30 Hz	8.2 %
$\delta\text{StarkTrap}$	0.0 Hz	0.0173 Hz	$\infty$	1.0	0.017 Hz	0.0 %
$\delta\text{relDopp}$	-0.01 Hz	$5.77 \cdot 10^{-3}$ Hz	$\infty$	1.0	$5.8 \cdot 10^{-3}$ Hz	0.0 %
$f_{\text{ZeemDC}}$	0.4965 Hz	0.0406 Hz				
$f_{\text{ZeemAC}}$	$10.4 \cdot 10^{-6}$ Hz	$12.0 \cdot 10^{-6}$ Hz				
s0	$52.00 \cdot 10^9$ Hz/T <sup>2</sup>	$2.60 \cdot 10^9$ Hz/T <sup>2</sup>	50	$9.5 \cdot 10^{-12}$	0.025 Hz	0.1 %
B <sub>DC</sub>	$3.09 \cdot 10^{-6}$ T	$100 \cdot 10^{-9}$ T	50	$320 \cdot 10^3$	0.032 Hz	0.1 %
B <sub>AC</sub>	$20.0 \cdot 10^{-9}$ T	$11.5 \cdot 10^{-9}$ T	$\infty$	not valid!	$12 \cdot 10^{-6}$ Hz	0.0 %
s3	0.0688 Hz/m	$577 \cdot 10^{-9}$ Hz/m	$\infty$	-0.75	$-430 \cdot 10^{-9}$ Hz	0.0 %
$h_{\text{refminusYb}}$	-0.75 m	$5.77 \cdot 10^{-3}$ m	$\infty$	0.069	$400 \cdot 10^{-6}$ Hz	0.0 %
$f_{\text{YbCorr}}$	0.4 Hz	1.05 Hz	60			

**Result:**Quantity:  $f_{\text{YbCorr}}$ **Value: 0.4 Hz****Expanded Uncertainty:  $\pm 2.1$  Hz**

Coverage Factor: 2.0

Coverage: t-table 95%

**Uncertainty Budget (2006 measurement):**

Quantity	Value	Standard Uncertainty	Degrees of Freedom	Sensitivity Coefficient	Uncertainty Contribution	Index
$f_{2ndZeem}$	0.3961 Hz	0.0349 Hz				
$f_{grav}$	-0.05625 Hz	$433 \cdot 10^{-6}$ Hz				
$\delta QShift$	0.0 Hz	1.00 Hz	50	1.0	1.0 Hz	90.8 %
$\delta Servo$	0.0 Hz	0.100 Hz	50	1.0	0.10 Hz	0.9 %
$\delta StarkBBD_{ev}$	0.0 Hz	0.300 Hz	50	1.0	0.30 Hz	8.2 %
$\delta StarkTrap$	0.0 Hz	0.0173 Hz	$\infty$	1.0	0.017 Hz	0.0 %
$\delta relDopp$	-0.01 Hz	$5.77 \cdot 10^{-3}$ Hz	$\infty$	1.0	$5.8 \cdot 10^{-3}$ Hz	0.0 %
$f_{ZeemDC}$	0.3961 Hz	0.0349 Hz				
$f_{ZeemAC}$	$10.4 \cdot 10^{-6}$ Hz	$12.0 \cdot 10^{-6}$ Hz				
$s_0$	$52.00 \cdot 10^9$ Hz/T <sup>2</sup>	$2.60 \cdot 10^9$ Hz/T <sup>2</sup>	50	$7.6 \cdot 10^{-12}$	0.020 Hz	0.0 %
$B_{DC}$	$2.760 \cdot 10^{-6}$ T	$100 \cdot 10^{-9}$ T	50	$290 \cdot 10^3$	0.029 Hz	0.1 %
$B_{AC}$	$20.0 \cdot 10^{-9}$ T	$11.5 \cdot 10^{-9}$ T	$\infty$	not valid!	$12 \cdot 10^{-6}$ Hz	0.0 %
$s_3$	0.0750 Hz/m	$577 \cdot 10^{-9}$ Hz/m	$\infty$	-0.75	$-430 \cdot 10^{-9}$ Hz	0.0 %
$h_{refminusYb}$	-0.75 m	$5.77 \cdot 10^{-3}$ m	$\infty$	0.075	$430 \cdot 10^{-6}$ Hz	0.0 %
$f_{YbCorr}$	0.3 Hz	1.05 Hz	60			

**Result:**Quantity:  $f_{YbCorr}$ **Value: 0.3 Hz****Expanded Uncertainty:  $\pm 2.1$  Hz**

Coverage Factor: 2.0

Coverage: t-table 95%